Suspended GaN beams and membranes on Si as a platform for waveguide-based THz applications

Downloaded from: https://research.chalmers.se, 2019-05-11 18:47 UTC

Citation for the original published paper (version of record):
Krause, S., Desmaris, V., Pavolotsky, A. et al (2018)
Suspended GaN beams and membranes on Si as a platform for waveguide-based THz applications
Journal of Micromechanics and Microengineering, 28(10)
http://dx.doi.org/10.1088/1361-6439/aacf5c

N.B. When citing this work, cite the original published paper.

research.chalmers.se offers the possibility of retrieving research publications produced at Chalmers University of Technology.
It covers all kind of research output: articles, dissertations, conference papers, reports etc. since 2004.
research.chalmers.se is administrated and maintained by Chalmers Library

(article starts on next page)

OPEN ACCESS
IOP Publishing

Journal of Micromechanics and Microengineering

J. Micromech. Microeng. **28** (2018) 105007 (7pp)

https://doi.org/10.1088/1361-6439/aacf5c

Suspended GaN beams and membranes on Si as a platform for waveguide-based THz applications

S Krause, V Desmaris, A Pavolotsky, D Meledin and V Belitsky

Group for Advanced Receiver Development, Chalmers University of Technology, SE-41296, Gothenburg, Sweden

E-mail: sascha.krause@chalmers.se

Received 7 March 2018, revised 15 June 2018
Accepted for publication 27 June 2018
Published 11 July 2018

Abstract

We demonstrate the suitability of employing suspended GaN beams on a Π-shaped Si frame for waveguide-based cryogenic THz components and systems. This concept addresses major challenges and provides eased device handling, cryogenic operation, micron-alignment possibilities, high integratability and allows the electrical contacting by using bonding wires. In particular, a balanced hot electron bolometer (HEB) mixer was implemented for frequencies at 1.3 THz with state-of-the-art IF performance, which combines micro-machined all-metal waveguide components in conjunction with a suspended GaN beam. In addition, in order to accomplish a proper design of active or passive components, the accurate knowledge of the effective dielectric constant at THz frequencies is crucial when such membranes are employed. Thus, a direct measurement method based on a resonance structure and an S-parameter measurement between 1 THz and 1.5 THz is also presented.

Keywords: THz components, GaN on Si, HEB, waveguide

(Some figures may appear in colour only in the online journal)

Introduction

The exploration of the THz frequency range is constantly gaining speed and numerous applications have emerged within research, security, astronomy, biomedicine and metrology in recent years [1–3]. The main reason for this relatively late development can be attributed to several technological challenges that had to be overcome. As the dimensions of microwave components usually scale with the wavelength, their size presents a serious issue when the device operation frequency is approaching the THz range. This manifests itself in certain performance limitations due to parasitic capacitances, thermal issues, the excitation of unwanted electromagnetic (EM) modes or excessive RF losses in conductors as the skin depth may approach the roughness of the metal surface. Waveguides for guiding THz EM waves offer wideband operation and full confinement of the fields, yet they are also miniaturized and demand high surface quality and accuracy on the waveguide dimensions and alignment. Several different micro fabrication techniques [4] were developed for this purpose and are based on copper electroforming over a thick sacrificial photo resist mold [5, 6] or deep Si etching processes [7]. In waveguide-based THz components, the actual substrate becomes more of a delicate membrane-like structure, which reduces the electrical loading of the waveguide and excludes substrate modes. However, it is difficult to manipulate and to place such beams suspended inside the waveguide with high alignment precision. Typically beam leads [8] made of thick electro-plated gold are used for the electrical contacting, however, once the device is mounted it can neither be modified nor removed in a non-destructive matter. One possible approach to overcome the aforementioned issues is based on a Π-shaped Si support frame holder [9], which keeps a thin Si membrane hosting the active device suspended. This concept has been successfully

Original content from this work may be used under the terms of the Creative Commons Attribution 3.0 licence. Any further distribution of this work must maintain attribution to the author(s) and the title of the work, journal citation and DOI.

© 2018 IOP Publishing Ltd Printed in the UK

implemented on a silicon-on-insulator (SOI) substrate as a technology demonstrator for a hot electron bolometer (HEB) mixer for the 1.6–2 THz frequency range [9], and provides easy handling, self-alignment, allows for cryogenic operation and can be electrically contacted with bonding wires despite a membrane thickness of only 2 μm. However, Si is often not the ideal choice of material for the beam as it may be incompatible with III–V device technologies, features a high dielectric constant of ε_r ~ 11.6 (1–3 THz) [10], and is not suitable for the deposition of high-quality single crystal superconducting thin films without using appropriate buffer-layers. Therefore, we suggest the use of GaN as the material for thin membranes, which has proven to be mechanically robust, inert to most chemicals, and allow for the growth of heterostructure and epitaxial nitrides [11, 12]. Furthermore, it has recently been demonstrated that GaN serves also as an excellent buffer-layer for the epitaxial growth of NbN superconducting nanofilms [13, 14], which are used in the most sensitive heterodyne receivers above 1.2 THz based on NbN HEB mixers for radio astronomical spectroscopy [15, 16]. Alternative buffer-layers or substrates that yield single crystal NbN films are MgO [17, 18], SiC [19, 20] and sapphire [21], however, the use of sapphire in waveguide applications is restricted due to its hardness and MgO as a thin buffer-layer on Si or lapped quartz substrates is hygroscopic and may lead to life-time issues in the active device. Moreover, they do not provide a good acoustic match to NbN thin films [22, 23], and results in a reduced phonon transparency, which has a negative impact on the achievable IF bandwidth in phonon-cooled HEB devices.

In this paper, we present the fabrication process for GaN/AlGaN suspended beams and membranes carrying the active device. In this regard, it is crucial for the proper design of RF circuits to have accurate knowledge of the dielectric constant of such epi-layer. A method is presented here that allows measuring the effective dielectric constant at THz using a resonance circuit, in particular a circular split ring resonator (SRR) and an S-parameter measurement setup.

Finally, we demonstrate the fabrication of a 1.3 THz balanced HEB mixer, which combines micro-machined all-metal waveguide components with a suspended GaN membrane on a supporting Si frame hosting the HEB mixer.

Device processing

The fabrication of the circuit to be implemented on the GaN membrane may vary substantially upon the respective application. However, it can generally be divided into the front-side processing of the device, the patterning of the beam and the subsequent backside etching to form a supporting Si frame for the suspended beam.

We demonstrate a waveguide-based NbN HEB mixer operating at 1.3 THz as the active device hosted by a suspended GaN beam as well as a SRR circuit on a freestanding GaN membrane to deduce its effective dielectric constant. The fabrication was based on a (1 1 1)-oriented 5-inch Si wafer of 1000 μm thickness with 3 μm AlGaN buffer-layer and 2.5 μm unintentionally doped GaN epi-layer, which is commercially available. Prior to processing, the wafer was diced into smaller specimen of approximately ½-inch × ½-inch sample size, whereas the Si was additionally thinned down to 90 ± 2 μm for the samples that were used for the fabrication of the HEB mixer.

Front-side processing of the NbN HEB mixer

The performance of HEB mixers is strongly linked to the structural and electrical properties of the used superconducting nanofilm, e.g. NbN. Thus, the deposition of the NbN film is usually the first process step and, in our case, was performed using DC magnetron sputtering in a reactive N_2/Ar gas atmosphere at elevated substrate holder temperature of 650 °C. The thickness of the NbN film is approximately 4.5 nm, and has been estimated from a calibrated specimen of 5 nm thickness and accordingly scaled deposition time. Hexagonal GaN (0 0 0 2) promotes the epitaxial growth of the superconducting NbN [13, 14], hence results in excellent superconducting properties such as low normal resistivity and a high critical temperature (T_c), which has been measured to be 12.8 K. In comparison, poly-crystalline films as they are obtained on e.g. bare Si substrates only exhibit T_c between 9–10 K [13, 24] for similar film thicknesses.

The HEB mixer comprises a submicron superconducting NbN bridge, which is confined by the gap between two normal metal contact pads. The bridge dimensions were varied from 0.1 × 1 μm to 0.4 × 3.6 μm to adjust the NbN bridge resistance to the designed impedance of the E-probe for optimized coupling of the THz radiation (figure 2(c)). E-beam lithography based on a ZEP 520A and a co-polymer lift-off system and evaporation of Ti (5 nm) as adhesion layer and Au (25 nm) were employed to define the contact pads and alignment marks, as it is illustrated in figures 1(a) and (b). The fabrication of separate and thin contact pads (figure 1(b)) is necessary to reduce parasitic capacitances across the NbN bridge, which otherwise would have a strong negative impact on the performance of the HEB at THz frequencies.

In a second E-lithography step (figure 1(c)), the remaining RF structure is formed such as the planar E-probe, RF choke filter and the bonding pads, which consist of an evaporated Au layer of 300 nm thickness (figure 1(d)). Lastly, the width of the bolometer was defined by a negative resist etching mask (figure 1(e)) and the subsequent removal of the uncovered NbN film in an inductively coupled plasma reactive ion etching process (ICP-RIE) (figure 1(f)) using CF_4 chemistry.

Suspended GaN beam and Si backside processing

The patterning of the GaN beam follows the front-side processing. The dimensions of the waveguide and waveguide channel, mostly determine the width and length of the GaN beam, respectively. Alignment notches, as illustrated in figure 2(c), were added to the beam design, and act primarily as a visual aid when placing and aligning the devices onto the waveguide opening.

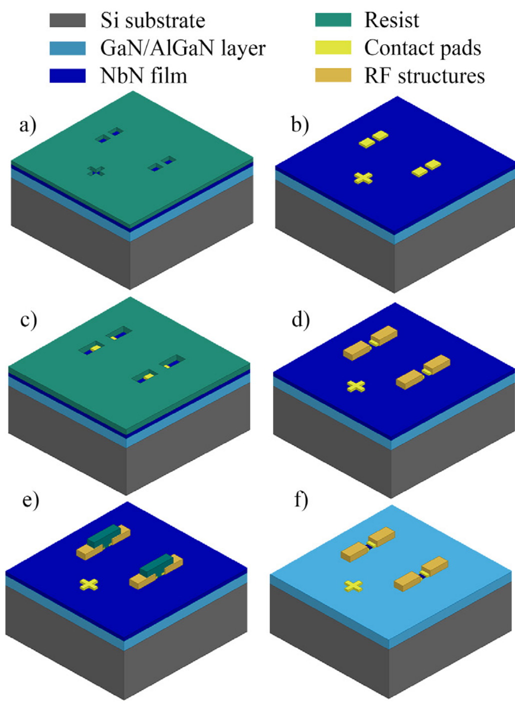

Figure 1. Front-side patterning of the thin NbN film towards a HEB with bridge dimensions of 0.1 × 1 μm to 0.4 × 3.6 μm (a) E-beam lithography of thin contact pads and alignment marks. (b) Evaporation of Ti/Au (5 nm/25 nm) and subsequent lift-off. (c) E-beam lithography of RF structures such as RF choke and E-probe (d) Evaporation of Ti/Au (5 nm/300 nm) and lift-off. (e) E-beam lithography using negative resist as etch mask for the definition of the bolometer width. (f) ICP-RIE etching for the removal of NbN, the superconducting bridge between the contact pads remains.

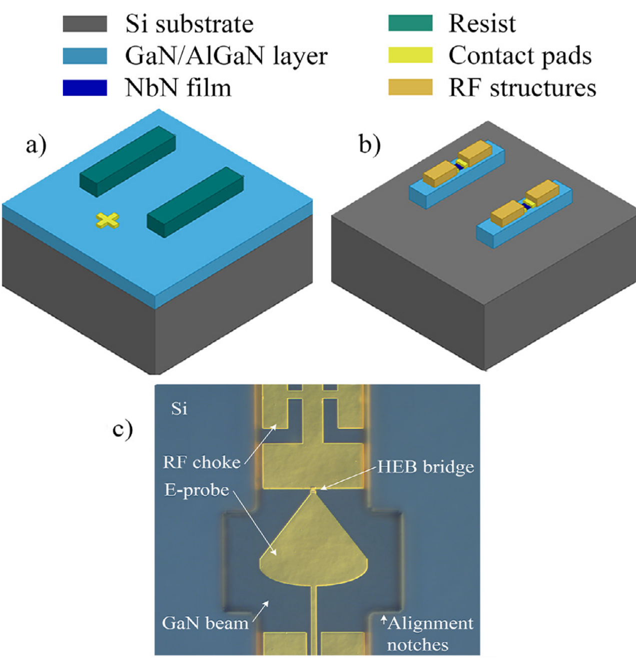

Figure 2. Definition of the GaN beams. (a) Using thick resist as etch mask, ICP RIE etching in CF_4/Ar. (b) HEB and RF structure hosted by a thin GaN membrane on a Si substrate. (c) Microscopy image of the device after the etching of the GaN/AlGaN layer.

The GaN beams were created by using a thick photo resist (AZ4562 of approximately 6.5–7 μm thickness), see figure 2(a), as an etch mask in an anisotropic chlorine-based etching process. The etch rate was approximately 150 nm min^{-1} and was achieved in an ICP RIE process with applied RF power of 100 W and a Cl_2/Ar gas mixture with gas flow of 30 sccm/15 sccm, respectively. The etching process through the entire GaN/AlGaN layer with total thickness of 5.5 μm has been monitored using a laser interferometer, which indicated when the underlying Si substrate was reached. Moreover, the applied process is highly selective to the Si substrate, and hence is very controllable and yielded a smooth surface, as depicted in figure 2(c).

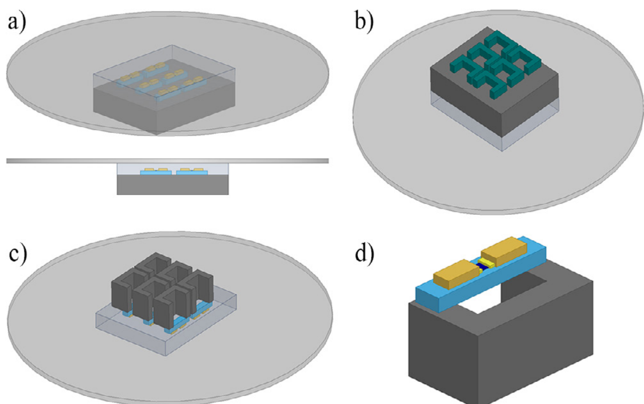

Figure 3. Backside patterning of the Si. (a) Mounting the chip upside down onto a 4-inch sapphire carrier wafer using a protective resist and a thermally resistant sacrificial layer. (b) Backside lithography using thick resist AZ 4562 as etch-mask. (c) Deep anisotropic silicon etching using the Bosch process. (d) Release of the carrier wafer, by dissolving the sacrificial layer and protective resist in a solvent. The separated devices can be transferred with a tweezer.

After patterning the GaN beam, the devices can easily be probed and characterized in order to monitor any degradation. The next process step consists of the patterning of the Si substrate from the back and will result in a suspended GaN beam. First, the chip was attached up-side down on a transparent sapphire carrier wafer using a protective photo resist and an adhesive sacrificial layer, as seen in figure 3(a). Backside photo lithography was employed to pattern the Π-shaped structure, which was then anisotropically etched following a Bosch process (figures 3(b) and (c)). The GaN layer itself acts as an etch stop in SF_6 chemistry, similarly to a silicon oxide layer when using a SOI wafer process. The separation of the individual devices was performed by removing the adhesion layer and photo resist in a solvent. The released devices were easy to handle with a tweezer despite the long and narrow (800 μm × 70 μm) suspended GaN beam, which is supported by the Si frame. After the release of the devices and their final sorting, the overall yield of the fabrication process and the handling procedure can be stated at approximately 82% (32 out of 39).

Waveguide micromachining and device packaging

The waveguide components were fabricated similarly to [5, 25], this micro machining method is based on copper electroforming over a sacrificial thick resist, which is patterned

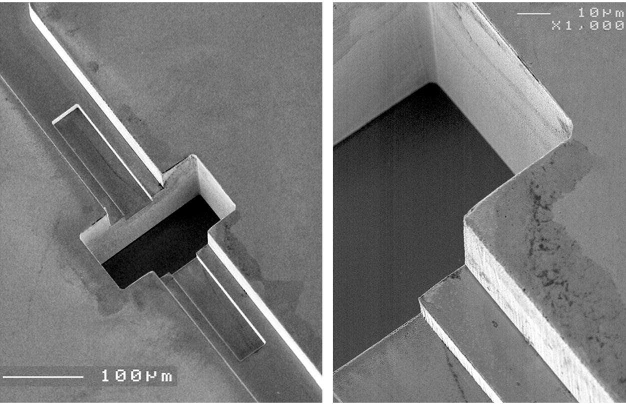

Figure 4. SEM image of the micro-machined waveguide components [5], in particular the waveguide back short and waveguide channel, which will host the suspended GaN beam. Note the excellent surface roughness and vertical sidewalls.

using photo lithography techniques. The surface roughness of the fabricated waveguide section employing this techniques is in the order of 20 nm. The individual HEB devices are placed onto the mixer block and are partly self-aligning due to the use of a surrounding Si frame that fits inside a recess. Figure 4 depicts the waveguide channel, in which the GaN beam hosting the HEB mixer, is placed.

The electrical contacting was realized by gold bonding wires that were directly applied onto the patterned and supported part of the GaN membrane and the all-metal mixer housing.

SRR design and fabrication

The accurate knowledge of the effective dielectric constant is crucial for the proper design of active or passive THz components. A resonance structure based on a SRR is employed to deduce the dielectric constant of the GaN/AlGaN membrane with a waveguide S-parameter measurement. The SRR is essentially a planar band-pass filter that can be modelled as an LC resonator. The inductance of the two interrupted rings in conjunction with the series capacitance formed by the gap yields a lumped resonator circuit, which can easily be miniaturized [26, 27]. The SRR is predominantly excited by a magnetic field, hence it can be positioned inside a rectangular waveguide to couple to the fundamental mode. Thus, the resonance feature of the SRR is embedded in the transmission characteristic of the waveguide, which can be measured and consequently be used to derive the dielectric properties of the membrane by using a 3D EM simulator such as *Ansys HFSS*.

The fabrication of the SRR was realized using E-beam lithography, evaporation of 300 nm Au and subsequent lift-off. The backside patterning of the SRR devices was not necessary, instead the bulk Si was removed completely in an ICP-RIE system in pure SF_6 gas and left a freestanding GaN membrane, which hosts the SRR. Figure 5 illustrates the used 3D model in the simulator *Ansys HFSS* and a SEM image of the mounted SRR inside the waveguide implemented in split-block technique.

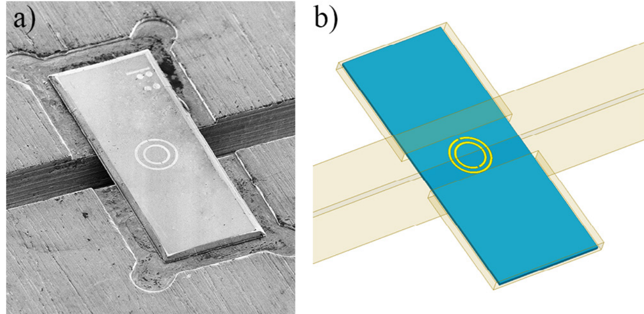

Figure 5. (a) SEM of the SRR structure on a freestanding GaN membrane mounted inside a straight waveguide section with dimensions of 165 × 83 μm. The bulk Si was removed completely from the backside by RIE in SF6. (b) EM 3D model of the SRR in *Ansys HFSS*, which was used for the design as well as for fitting the dielectric constant of the membrane to match the measurement data.

Results and discussion

Dielectric constant of the GaN/AlGaN membrane

The waveguide block hosting the SRR device was measured by a calibrated VNA extension module setup between 1 THz to 1.5 THz. The standing wave pattern in the measurement data reveals that the alignment between VNA unit and waveguide section was not ideal, however, it was possible to implement this misalignment in the 3D full wave simulation. The dielectric constant of the membrane determines the frequency of the resonance feature and was used as a fitting parameter until good agreement between measurement and simulation data was achieved, as it is illustrated in figure 6. The discrepancy in the amplitude of the standing waves can be explained with uncertainties in the exact knowledge of electrical conductivity in the waveguide walls and SRR structure, and with the challenges that are associated with the VNA calibration at THz frequencies. However, the simulation data also confirms that the amplitude is not affecting the resonance feature. The best fit was obtained for a permittivity of $\varepsilon_r = 4.9 \pm 0.15$, which can be considered as the effective dielectric constant of the GaN layer and AlGaN buffer-layer. The literature value for GaN and AlN in the high frequency limit is ranging from 5.35–5.8 and 4.16–4.84, respectively, depending on the E-field polarization and temperature [28–32]. This is consistent with our experimentally measured value of the GaN/AlGaN stack at 1.3 THz.

The presented technique of deriving the dielectric constant from an S-parameter measurement at THz frequencies can be seen as a viable alternative to THz time domain spectroscopy (TDS). However, a more complex resonance structure would be needed to deduce the dielectric properties over a wider frequency range. It should be emphasized that the dielectric properties of GaN experience a relatively strong frequency dependence when compared to Si, whose THz permittivity of ~11.6 [10] is similar to its value at static electrical fields and this, in fact motivates the need for such characterization technique for a particular material combination and frequency range.

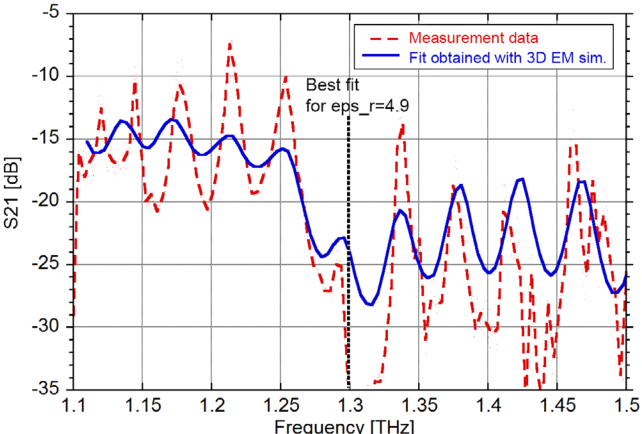

Figure 6. THz transmission measurement and simulation data of the SRR devices inside a straight waveguide section. The standing waves are an artefact of the misalignment between the waveguide section and the VNA extension module output waveguide. The resonance at 1.3 THz has been reproduced in the simulator and corresponds to a dielectric constant of 4.9.

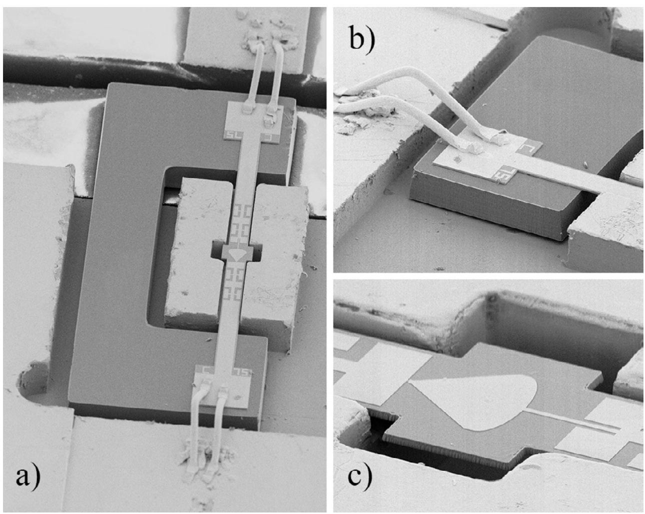

Figure 7. SEM images of the mounted HEB mixer on the micro-machined all-metal block. (a) An excess in the block accommodates the Π-shaped bulk Si frame, the GaN beam hosting the HEB device is suspended and lies inside the wave channel. (b) Electrical contacting using gold bonding wires is possible due to the rigid bulk Si underneath the bonding pads. (c) The E-probe and HEB bridge aligned inside the waveguide opening. The extending notches facilitate the alignment precision and limit the maximum misalignment.

The GaN membrane is especially beneficial over Si in waveguide-based THz applications due to lower capacitive loading, which should be advantageous from a design perspective as well as allows for thicker substrates that provide additional mechanical stability and more effective cooling for active devices.

Balanced waveguide heterodyne receiver at 1.3 THz

The NbN HEB mixer on the GaN beam was mounted into a recess of the micro machined block that accommodates the Π-shaped bulk Si frame, as seen in figure 7(a). The latter gives enough rigidity to use gold bonding wires (figures 7(a) and (b)) for the electrical contacting of the device, which is compliant with space standards.

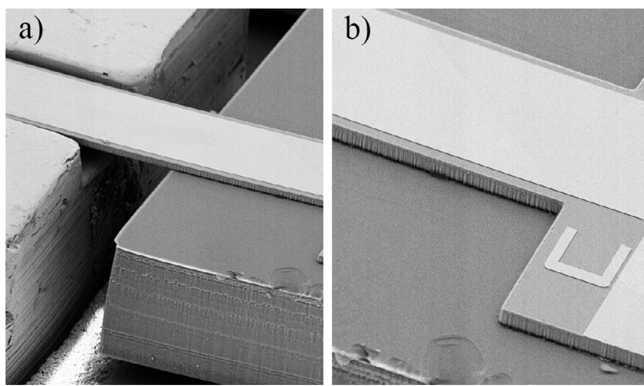

Figure 8. SEM of the suspended GaN beam: (a) inside the waveguide channel and (b) the GaN beam with metallization on the supporting bulk Si.

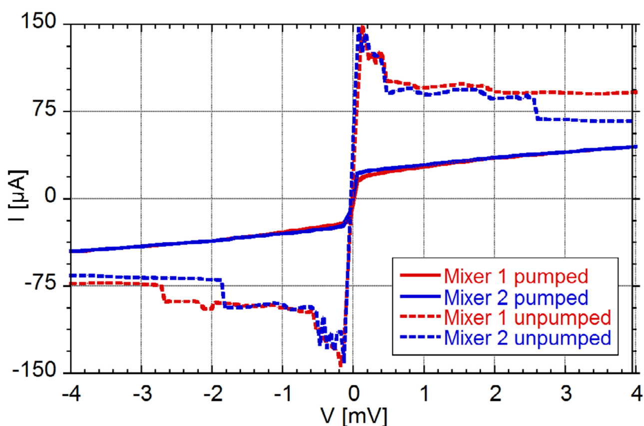

Figure 9. Current–voltage characteristics of the HEB mixers used in the balanced receiver layout. Their critical current is almost identical and amounts to 150 μA. Upon applied LO signal, both mixers are pumped equally, which implies that they have been aligned optimally inside the waveguide.

Figure 7(c) demonstrates the alignment accuracy of the E-probe inside the waveguide, which is critical for coupling the THz signal optimally to the HEB bridge. The alignment notches provide visual guidance and limit the maximum misalignment. The suspended GaN beam features almost vertical sidewalls, whereas the Si surface appears smooth, as it is illustrated in figures 8(a) and (b).

The balanced receiver scheme offers several advantages over the single-ended mixer configuration such as all available LO power can be utilized and it ideally provides immunity to amplitude modulations from the LO source [33], which is predominantly limiting the stability of HEB receivers [34]. However, the balanced configuration is more complex than its single-ended counterpart and comprises of a RF hybrid, which combines the RF and LO single, two HEB mixers, which ideally exhibit identical electrical properties, and an in-phase IF combiner [30]. One pair of HEBs with 0.2×1.6 μm bridge dimensions are used for the characterization at 1.3 THz local oscillator (LO) frequency and their current–voltage characteristics (IVC) are depicted in figure 9. Without applied LO

signal, they feature a critical current (I_c) measured at 4.6 K bath temperature of ~150 μA, which is almost identical for both HEB devices and implies that advantages associated with the balanced scheme can be fully utilized. Moreover, upon applied LO it was possible to pump the HEBs equally (figure 9), which is evidence of their accurate mounting and alignment inside the waveguide.

The HEB mixers have been subjected to several coolings and warm-ups (five in total) in a series of characterizations without any degradation of their electrical properties such as the critical current. This supports their mechanical robustness as fragile devices tend to break on the first cooling to cryogenic temperatures to our experience.

The results of the RF characterization at 1.3 THz of the full heterodyne receiver are presented in [35] and show a significantly enhanced noise bandwidth of 7 GHz due to the employment of the GaN buffer-layer, in comparison to typically 3.5 GHz achieved for state-of-the-art receivers based on NbN-on-Si HEB mixers [15, 36] with similar sensitivity or noise temperature. The limited IF bandwidth of NbN HEB mixers has previously been the main concern and can significantly be extended with the use of the GaN buffer-layer.

The concept of GaN on a supporting Si frame can be employed on prospective multi-pixel receiver applications due to the improved performance, easy handling of individual devices, excellent electrical contacting and possibility to further integrate the GaN platform with passive or active IF circuitry.

Conclusion

The use of a suspended GaN beam on a supporting Π-shaped Si frame for a waveguide THz HEB mixer with state-of-the-art IF performance was demonstrated. The patterning of the GaN beam as well as the Si backside was reliably performed by using anisotropic RIE-ICP etching processes in either chlorine or SF_6 chemistry, respectively. The concept addresses major challenges that are common to THz components due to the small device dimensions. The supporting Si frame allows for easy handling, operation at cryogenic temperatures, micron alignment possibilities as well as the electrical contacting using bonding wires. Also crucial for the proper design of THz components is the accurate knowledge of effective dielectric constant of the membrane used to fabricate the device on. A direct measurement method based on a resonance structure and a S-parameter measurement between 1 and 1.5 THz is presented and suggests a dielectric constant of 4.9 for the GaN/AlGaN membrane at 1.3 THz. The low permittivity compared to Si should have positive implications for the wideband design of waveguide based THz components. Moreover, the GaN membrane on Si material platform can be complemented with a doped AlGaN heterostructure, and opens the possibility for a high level of integration with other technologies combined with the possible operation in harsh environments.

Acknowledgment

The authors would like to acknowledge S-E Ferm for the fine-machining of waveguide components.

ORCID iDs

S Krause https://orcid.org/0000-0003-0164-3131
V Desmaris https://orcid.org/0000-0002-2246-9884
A Pavolotsky https://orcid.org/0000-0001-9336-4601
V Belitsky https://orcid.org/0000-0003-0502-6261

References

[1] Mittleman D M 2017 Perspective: terahertz science and technology *J. Appl. Phys.* **122**

[2] Sun Q, He Y, Liu K, Parrott E P J and Pickwell-MacPherson E 2017 Recent advances in terahertz technology for biomedical applications *Quant. Imaging Med. Surg.* **7** 345–55

[3] Rogalski A and Sizov F 2011 Terahertz detectors and focal plane arrays *Opto-Electron. Rev.* **19** 346–404

[4] Chattopadhyay G, Reck T, Lee C and Jung-Kubiak C 2017 Micromachined packaging for terahertz systems *Proc. IEEE* **105** 1139–50

[5] Desmaris V, Meledin D, Pavolotsky A, Monje R and Belitsky V 2008 All-metal micromachining for the fabrication of sub-millimetre and THz waveguide components and circuits *J. Micromech. Microeng.* **18** 095004

[6] Pavolotsky A, Meledin D, Risacher C, Pantaleev M and Belitsky V 2005 Micromachining approach in fabricating of THz waveguide components *Microelectron. J.* **36** 683–6

[7] Jung-Kubiak C, Reck T, Alonso M and Chattopadhyay G 2016 Silicon micromachined components at 1THz and beyond *41st Int. Conf. on Infrared, Millimeter, and Terahertz waves (IRMMW-THz) (Copenhagen)*

[8] Bass R B, Schultz J C, Lichtenberg A W, Kooi J W and Walker C K 2003 Beam lead fabrication for submillimeter-wave circuits using vacuum planarization *14th Int. Symp. on Space Terahertz Technology (Tucson, USA)*

[9] Dochev D, Desmaris V, Pavolotsky A, Meledin D and Belitsky V 2011 A technology demonstrator for 1.6-2 THz waveguide HEB receiver with a novel mixer layout *J. Infrared Millim. Terahertz Waves* **32** 451

[10] Bolivar P H, Brucherseifer M, Rivas J G, Gonzalo R, Ederra I, Reynolds A L, Holker M and Maagt P D 2003 Measurement of the dielectric constant and loss tangent of high dielectric-constant materials at terahertz frequencies *IEEE Trans. Microw. Theory Tech.* **51** 1062–6

[11] Morkoc H 2008 *Handbook of Nitride Semiconductors and Devices* (Weinheim: Wiley)

[12] Yang Z, Wang R N, Jia S, Wang D, Zhang B S, Lau K M and Chen K J 2006 Mechanical characterization of suspended GaN microstructures fabricated by GaN-on-patterned-silicon technique *Appl. Phys. Lett.* **88** 041913

[13] Krause S, Meledin D, Desmaris V, Pavolotsky A, Belitsky V, Rudzinski M and Pippel E 2014 Epitaxial growth of ulta-thin NbN films on $Al_xGa_{1-x}N$ buffer-layers *Supercond. Sci. Technol.* **27** 065009

[14] Krause S, Afanas'ev V, Desmaris V, Meledin D, Pavolotsky A, Belitsky V, Lubenschenko A, Batrakov A, Rudzinski M

and Pippel E 2016 Ambient temperature growth of mono- and polycrystalline NbN nanofilms and their surface and composition analysis *Appl. Supercond.* **26** 7500205
[15] Risacher C *et al* 2015 First supra-THz heterodyne array receivers for astronomy with the SOFIA observatory *IEEE Trans. Terahertz Sci. Technol.* **6** 199–211
[16] Meledin D *et al* 2009 A 1.3-THz balanced waveguide HEB mixer for the APEX telescope *IEEE Trans. Microw. Theory Tech.* **57** 89–98
[17] Kang L, Jin B, Liu X, Jia X and Chen J 2011 Suppression of superconductivity in epitaxial NbN ultrathin films *J. Appl. Phys.* **109**
[18] Meledin D, Tong E, Blundell R, Kaurova N, Smirnov K, Voronov B and Gol'tsman G 2003 Study of the IF bandwidth of NbN HEB mixers *Appl. Supercond.* **13** 164–7
[19] Dochev D, Desmaris V, Pavolotsky A, Meledin D, Lai Z, Henry A, Janzen E, Pippel E, Woltersdorf J and Belitsky V 2011 Growth and characterization of epitaxial ultra-thin NbN films on 3C-SiC/Si substrates for terahertz applications *Supercond. Sci. Technol.* **24** 035016
[20] Gao J, Hajenius M, Tichelaar F, Klapwijk T, Voronov B, Grishin E, Gol´tsman G, Zorman C and Mehregany M 2007 Monocrystalline NbN nanofilms on a 3C-SiC/Si substrate *Appl. Phys. Lett.* **91** 062504
[21] Lamaestre R E D, Odier P, Bellet-Amalric E, Cavalier P, Pouget S and Villegier J-C 2007 High quality ultrathin NbN layers on sapphire for superconducting single photon detectors *J. Phys.: Conf. Ser.* **97** 012046
[22] Kaplan S B 1979 Acoustic matching of superconducting films to substrates *J. Low Temp. Phys.* **37** 343–64
[23] Krause S, Mityashkin V, Antipov S, Gol'tsman G, Meledin D, Desmaris V, Belitsky V and Rudzinski M 2017 Reduction of phonon escape time for NbN hot electron bolometers by using a GaN buffer layers *IEEE Trans. Terahertz Sci. Technol.* **7** 53–9
[24] Ilin K, Schneider R, Gerthsen D, Engel A, Bartolf H, Schilling A, Semenov A, Huebers H-W, Freitag B and Siegel M 2008 Ultra-thin NbN films on Si: crystalline and superconducting *J. Phys.: Conf. Ser.* **97** 012045
[25] Desmaris V, Meledin D, Dochev D, Pavolotsky A and Belitsky V 2011 Terahertz components packaging using integrated waveguide technology *IEEE MTT-S Int. Microwave Workshop on Millimeter Wave Integration Technologies* pp 81–4
[26] Baena J *et al* 2005 Equivalent-circuit models for split-ring resonators and complementary split-ring resonators coupled to planar transmission lines *IEEE Trans. Microw. Theory Tech.* **53** 1451–61
[27] Bonache J, Gil I, Garcia-Garcia J and Martin F 2005 Complementary split rings resonators (CSRRs): towards the miniaturization of microwave device design *J. Comput. Electron.* **5** 193–7
[28] Bougrov V, Levinshtein M E, Rumyantsev S L and Zubrilov A 2001 *Properties of Advanced Semiconductor Materials GaN, AlN, InN, BN, SiC, SiGe* (New York: Wiley)
[29] Barker A S and Ilegems M 1973 Infrared lattice vibrations and free-electron dispersion in GaN *Phys. Rev.* B **7**
[30] Manchon J D D, Dean J A S and Zetterstrom R B 1970 *Solid State Commun.* **8**
[31] Collins A T, Lightowlers E C and Dean P J 1967 *Phys. Rev.* **3** 833–8
[32] Moore W J, Freitas J A, Holm R T, Kovalenkov O and Dmitriev V 2005 Infrared dielectric function of wurtzite aluminium nitride *Appl. Phys. Lett.* **86** 141912-1–3
[33] Kooi J, Chamberlin R, Monje R, Force B, Miller D and Phillips T 2012 Balanced receiver technology development for the caltech submillimeter observatory *IEEE Trans. Terahertz Sci. Technol.* **2** 71–84
[34] Kooi J W, Baselmans J J A, Baryshev A, Schieder R, Hejnius M, Gao J, Klapwijk T M, Voronov B and Gol'tsman G 2006 Stability of heterodyne terahertz receivers *J. Appl. Phys.* **100** 064904
[35] Krause S, Meledin D, Pavolotsky A, Desmaris V, Rashid H and Belitsky V 2018 Noise and IF gain bandwidth of a balanced waveguide NbN/GaN hot electron bolometer mixer operating at 1.3 THz *IEEE Trans. Terahertz Sci. Technol.* **8** 365–71
[36] de Graauw T *et al* 2010 The Herschel-heterodyne instrument for the far-infrared (HIFI) *Astron. Astrophys.* **518**